Supporting Information

Crystallization induced phase separation: a unique tool to design microfiltration membranes with high flux and sustainable antibacterial surface

Maya Sharma[1], Sanjay Remanan[2], Giridhar Madras[3] and Suryasarathi Bose[2*]

[1]Center for Nano Science and Engineering, [2]Department of Materials Engineering,
[3]Department of Chemical Engineering, Indian Institute of Science, Bangalore-560012, India.

Selective etching of PMMA from PVDF/PMMA blend: assessed using TGA and DSC

Further confirmation of PMMA removal came from DSC measurements, as shown in Figure S1. In DSC thermographs of 50/50 blends, before etching, two glass transition (T_g) temperatures were noted (the lower one corresponds to PVDF and one at a higher temperature at ca. 57 ^oC corresponds to PMMA), whereas a single T_g was observed after etching. This clearly shows that PMMA phase has been completely etched out from the blends. This was confirmed in all the blend compositions studied here and is shown in Figure S1.

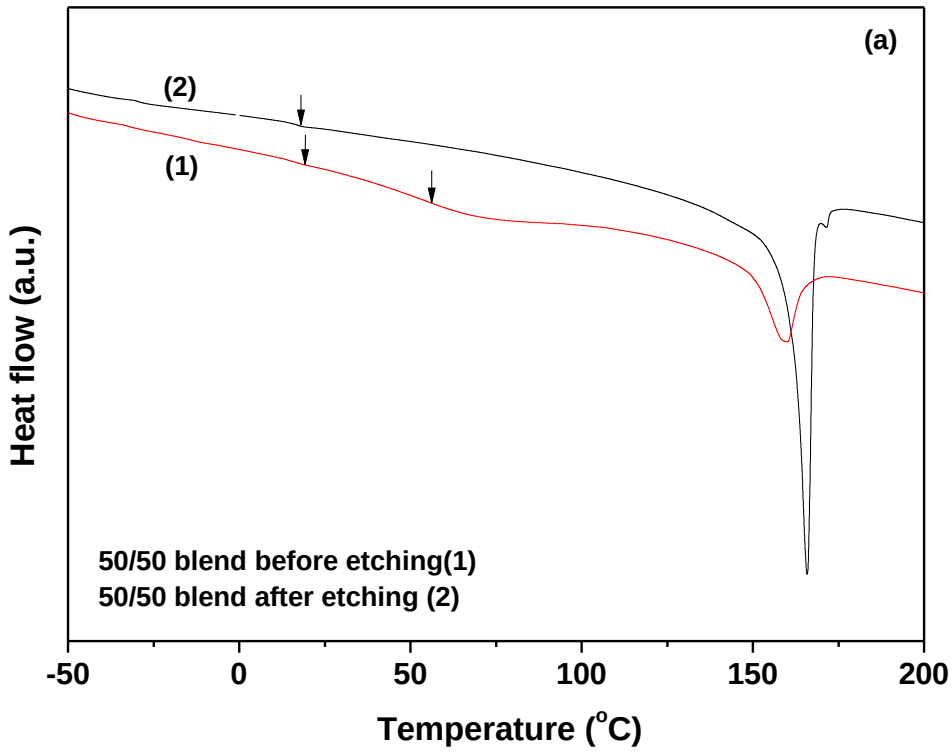
(a)
(2)
(1)
Heat flow (a.u.)
50/50 blend before etching(1)
50/50 blend after etching (2)
-50
0
50
100
150
200
Temperature (°C)

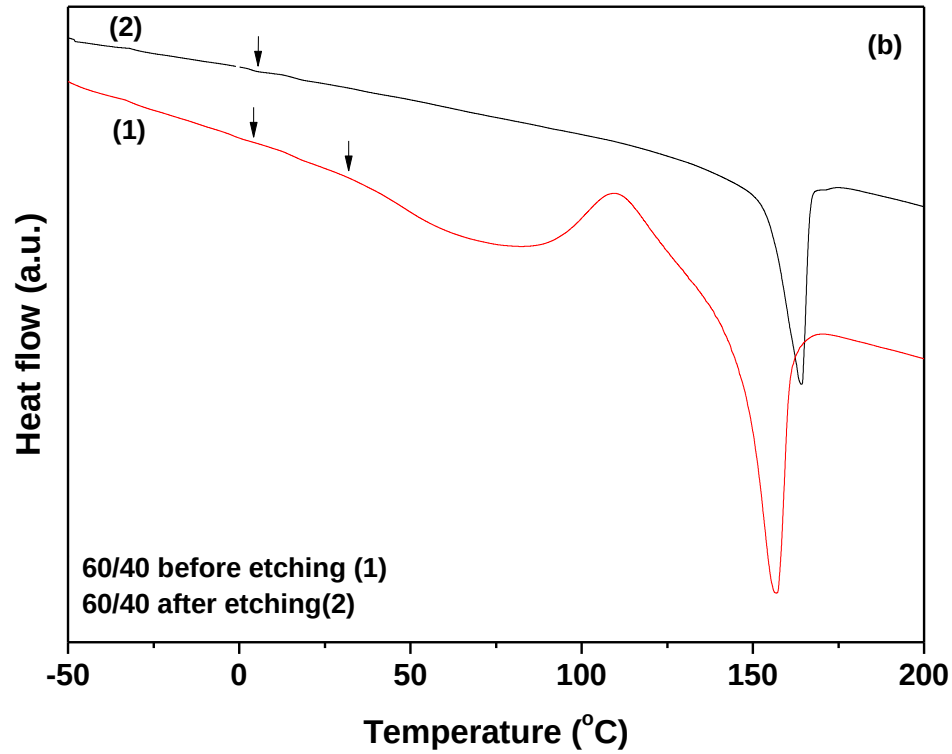
(b)
(2)
(1)
Heat flow (a.u.)
60/40 before etching (1)
60/40 after etching(2)
-50
0
50
100
150
200
Temperature (°C)

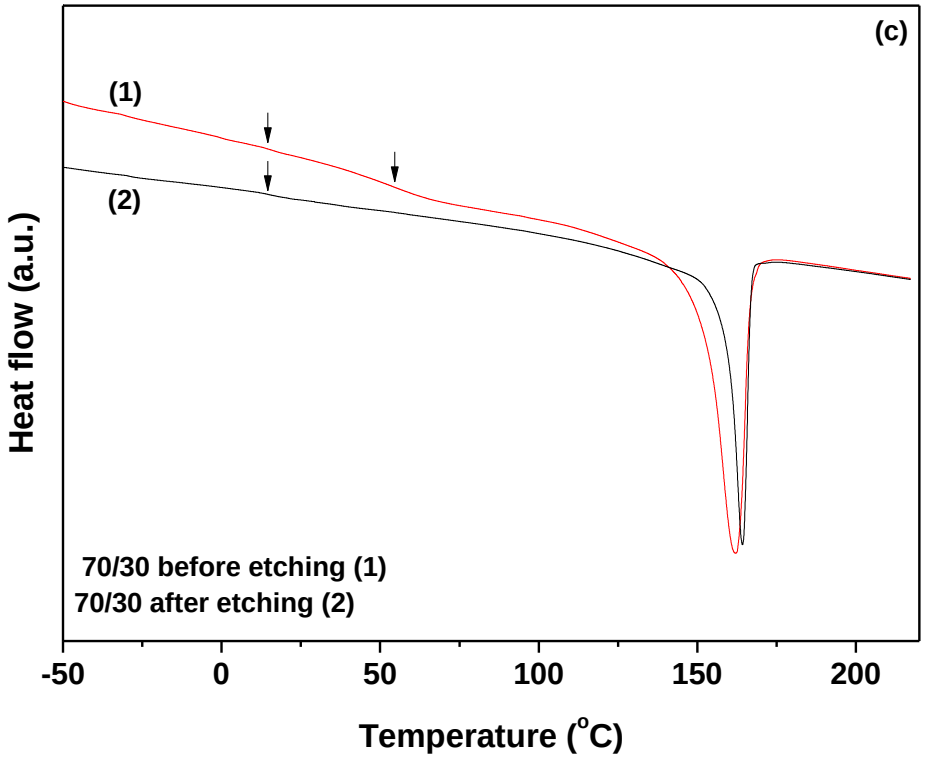
(c)
(1)
(2)
Heat flow (a.u.)
70/30 before etching (1)
70/30 after etching (2)
-50
0
50
100
150
200
Temperature (°C)

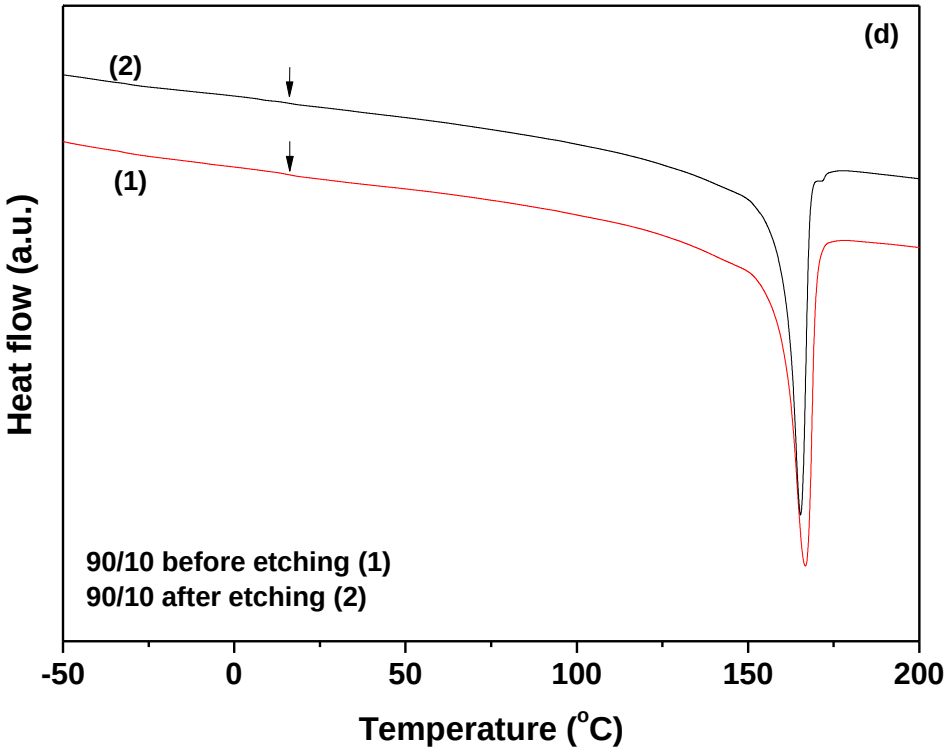
(d)
(2)
(1)
Heat flow (a.u.)
90/10 before etching (1)
90/10 after etching (2)
-50
0
50
100
150
200
Temperature (°C)

Figure S1: DSC profile of blends before and after etching PMMA from PVDF/PMMA blends, (a) 50/50, (b) 60/40, (c) 70/30, and (d) 90/10 blends.

Roughness of membranes

Figure S2 displays the three-dimensional AFM height images of the different nanoporous membranes. The surface roughness (R_a) of the membranes in a scan area of 25 μm × 25 μm is also shown. As reported, roughness commonly lead to two changes in the membrane; an increase of efficient filtration area and a decrease of the anti-fouling performance. Figure S2 demonstrates tapping mode AFM images of etched PVDF/PMMA membranes for the three compositions: 60/40, 70/30 and 90/10, respectively.

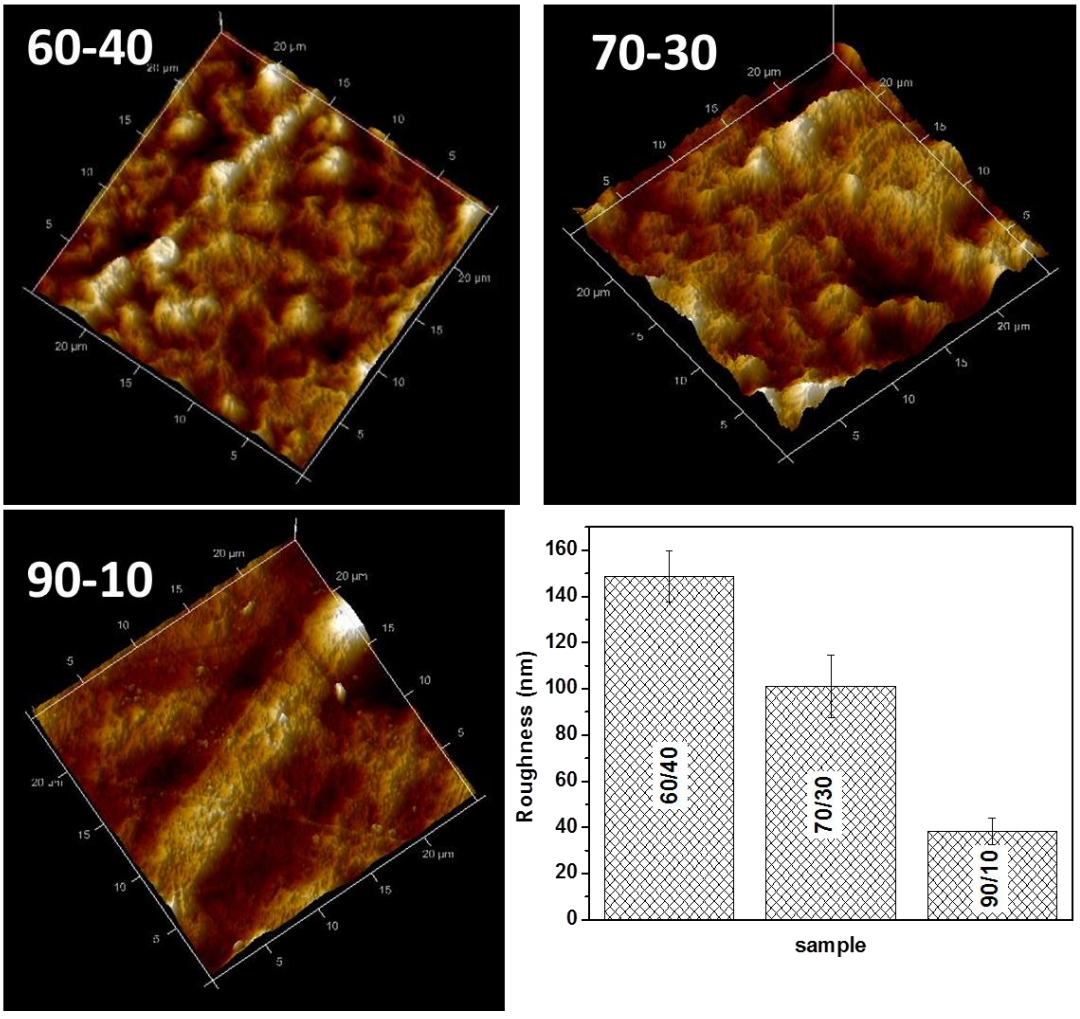

Figure S2: AFM 3-dimensional height surface images of membranes: 60/40, 70/30 and 90/10 PVDF/PMMA respectively and quantitative surface roughness of membranes obtained from AFM experiments.

The observed roughness of 90/10 blend is 38 (±5) nm as compared to 101 (±13) nm and 148 (±11) nm for 70/30 and 60/40 membranes, respectively.

Water contact angle

The variation of the static water contact angle of the etched and unetched token PVDF/PMMA blend is illustrated in Figure S3. The unetched membranes exhibited similar water contact angles of 75°± 2°, which is higher than that of etched membranes. The maximum difference in contact angle before and after etching is observed in 60/40 PVDF/PMMA blends. These results are in harmony with AFM results where 60/40nanoporous membranes showed maximum surface roughness (148 nm). As the roughness of the membrane increases, the hydrophilicity of the membranes also increases and thereby decreases the water contact angle.

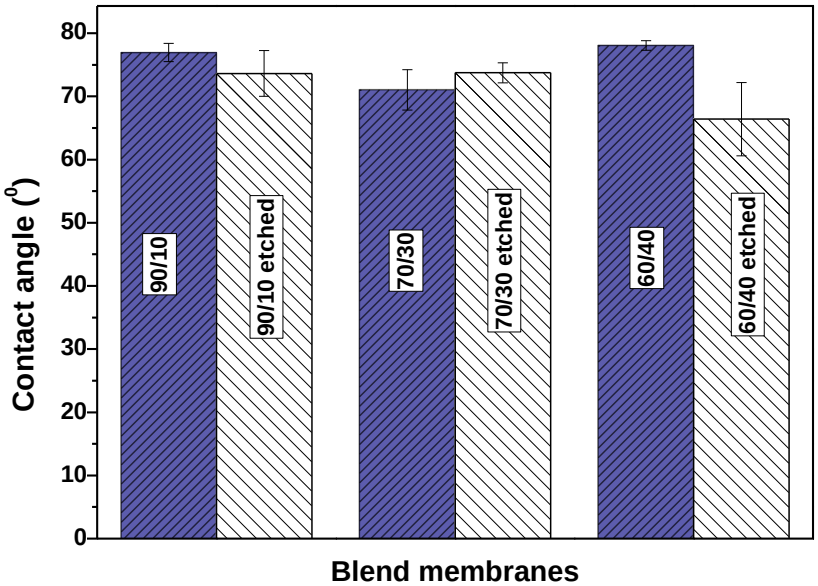

Figure S3: Water contact angle of PVDF/PMMA blend with and without PMMA etching.

Process governed gradient in morphology in PVDF/PMMA films prepared using compression molding

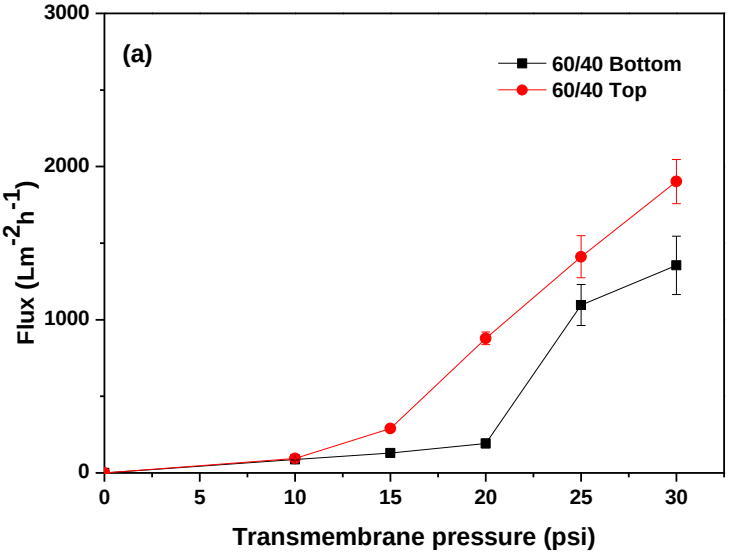

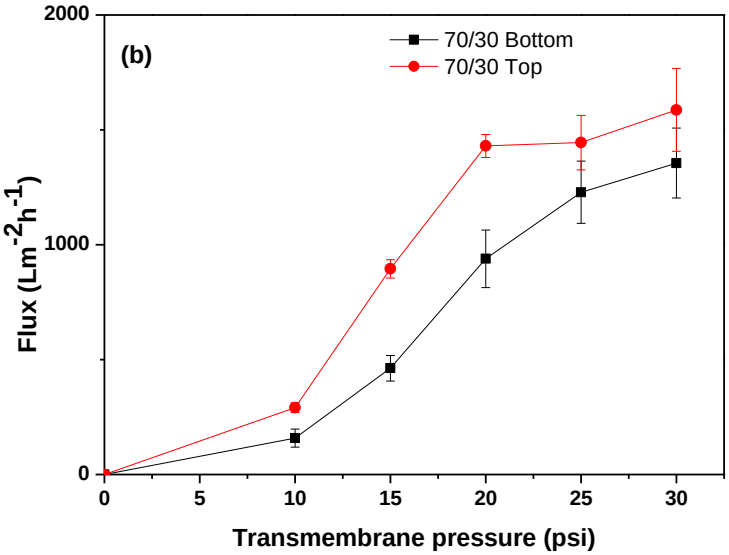

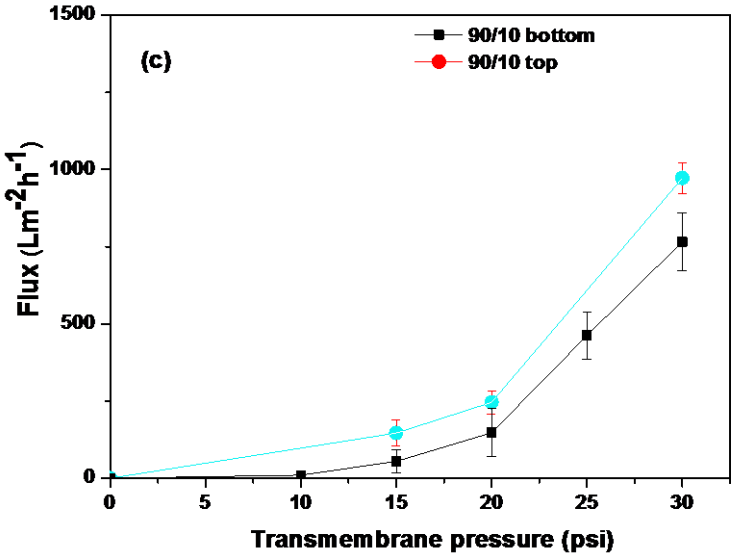

Figure S4: Flux at various transmembrane pressure level for (a) 60/40, (b) 70/30 and (c) 90/10 PVDF membranes

Further, to observe the effect of compositional difference on both sides, flux was evaluated by reversing the sides, as illustrated in Figure S4. There is a small difference in transmembrane flux on both sides. This difference in flux is possibly due to the difference in composition and the crystalline morphology as explained by concentration gradient formed in membranes. For instance, in 60/40 PVDF/PMMA porous membranes, one surface shows higher flux (1900±140 $Lm^{-2}h^{-1}$) than the other side (1350±190 $Lm^{-2}h^{-1}$) at a given pressure (here 30 psi). Similarly, 70/30 membranes showed slightly higher flux when the sides were reversed. The 90/10 membranes showed the least flux as compared to other compositions due to smaller pore size.

PVDF/PMMA blends were melt-mixed at 220°C for 20 minutes at 60 rpm. The extruded strands were used to compression mould into token disks followed by etching with acetic acid to design porous structures. The morphological analysis was done to gain in-depth understanding of the gradient in morphology due to differential spherulitic distribution in the

token membranes. There is a possibility of gradient in morphology during compression molding as the rheology of the phases are quite different (the zero shear viscosities are η_{PMMA} = 9885 Pa s and η_{PVDF} = 32835 Pa s). This hypothesis was confirmed by XPS measurements performed on both the sides of the token membranes (provided in supplementary information). Scheme S1 shows a cartoon illustrating the difference in C/F ratio on the both sides of the films. This difference can be explained based on the rheology of the phases which results in PVDF rich on one side and lean on the other. It appears that PMMA spreads more on one side of the token membrane in contrast to the other side. Such a difference in spreading has been observed earlier in PE/PEO blends and has been confirmed using acoustic scanning electron microscopy[26]. Presumably, during compression molding, the less viscous PMMA phase spreads more, while the higher viscous PVDF spreads less during molding. This leads to a gradient in the morphology of the sample and the concentration of PVDF is different on both sides as confirmed by XPS (see Figure S5). This possibly could be one of the reasons behind the different surface concentration, morphology and flux differences in the PVDF/PMMA blends.

Figure S5 depict the C 1s spectra taken from the both sides of 50/50 and 90/10 PVDF/PMMA films, respectively. In the XPS spectra of 50/50 PVDF/PMMA films, the C 1s spectrum can be deconvoluted into 5 distinct peaks at 285 (-CH2, -CH3), 285.9 (-C-), 286.8 (-OCH3), 289.1 (-COO-) and 290.8 eV (-CF2-). Specifically, peaks at 290.8 and 289.1 eV can be used to calculate PVDF and PMMA contents. As depicted in Figure S5 a-b, both the sides reflected in different C/F ratio. For instance, on one side it is 8.85 as compared to another side which is 12.34. This difference can be explained based on the rheology of the phases which results in PVDF rich on one side and lean on the other. Elemental carbon spectrum of 90/10 blend is different from 50/50 blend, specifically when considered 289.1 (-COO-) and 290.8 eV (-CF2-) binding energies. This can be due to lower concentration of PMMA in the

blend. The C1s spectrum can be deconvoluted into 4 peaks centered at 285 (-CH2, -CH3), 289.1 (-COO-) and 290.4 eV (-CF2-). The concentration difference on both side of the token membranes is quite significant in 90/10 blends. The atomic concentration (C/F) ratio on both sides is 3.33 as compared to another side which is 6.79. As the concentration of one polymer is higher than the other (here PMMA), the spreading of these phases during compression molding is quite different. Presumably, during compression molding, the less viscous PMMA (η_{PMMA} = 9885 Pa s) phase spreads more, while the higher viscous PVDF (η_{PVDF} = 32835 Pa s) spreads less during molding. This leads to a gradient in the morphology of the sample and the concentration of PVDF is different on both sides as confirmed by XPS.

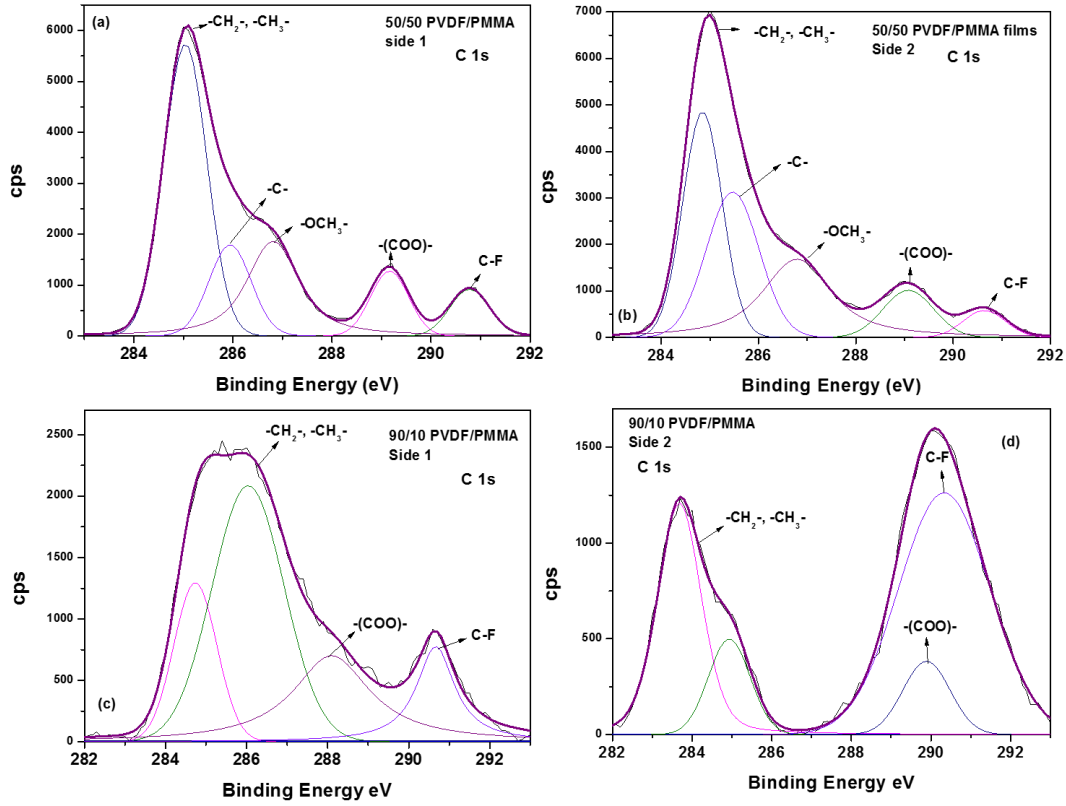

Figure S5: C 1s core level XPS spectrum of PVDF/PMMA blends (a) 50/50 side 1, (b) 50/50 side 1, (c) 90/10 side 1 and (d) 90/10 side 2.

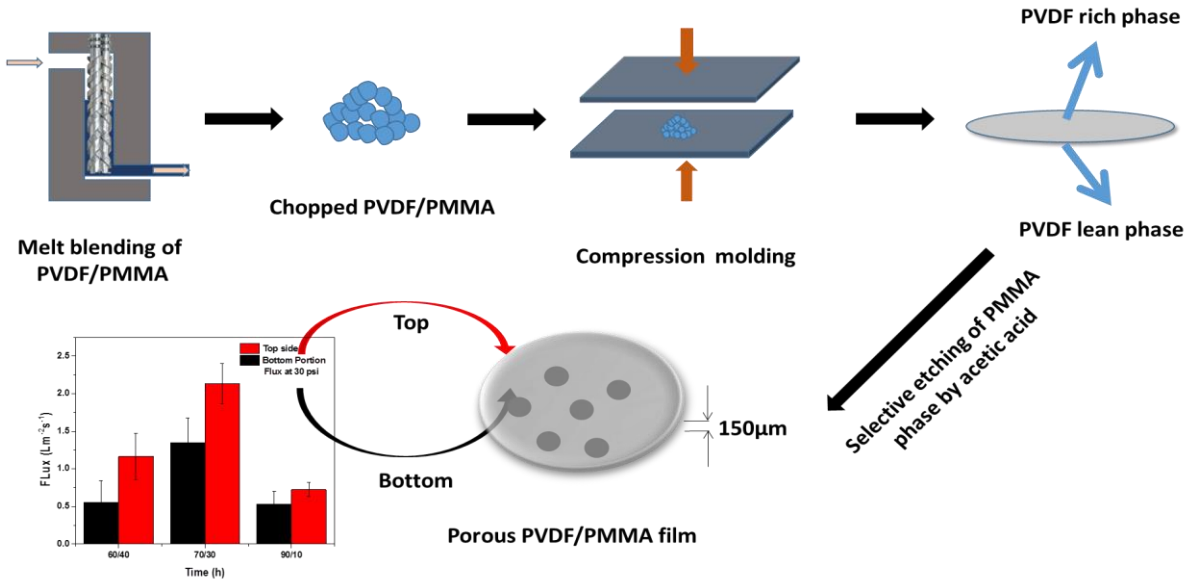

Scheme S1: A cartoon illustrating the membrane preparation and difference in surface topography of membrane.

Membrane Compaction

Experiments were performed to understand the compaction in the designed token membranes. Experiments were performed by running the same membrane in a cross flow cell for eight hours (at 30 psi pressure) for successive three days. Figure S6 shows the permeate flux as a function of time for all PVDF membranes. It shows the variation in permeate flux with time during the experiment. There was a drop in permeate flux and it remained constant during the rest of the test reaching a pseudo-steady state. Flux of the membranes decreased with respect to time indicating that pores are compacted during the experiment. During the first day of experiment, all membranes showed considerable initial flux compared to second day and it further decreased on day three. Among all the membranes, 60/40 membranes had higher flux during initial hours of experiment. Initial permeate flux of 60/40 token membranes was about 1742±145 $Lm^{-2}h^{-1}$, reduced to 1440±130 $Lm^{-2}h^{-1}$ (at the end of first day) and after 3 days eventually saturated to about 366±80 $Lm^{-2}h^{-1}$. 70/30 token membranes also showed similar

trend as that of 60/40 membrane. However, in the case of 90/10 membranes, an irregular pattern is observed at the end of third day and the permeate flux decreased.

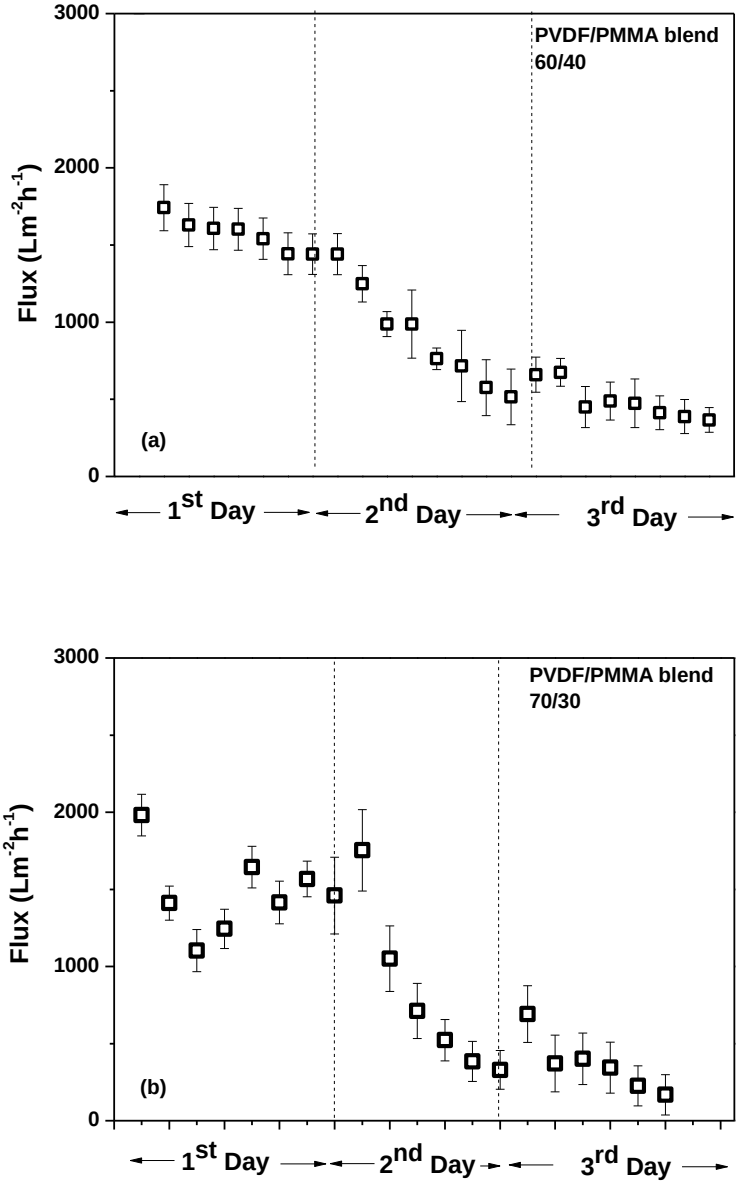

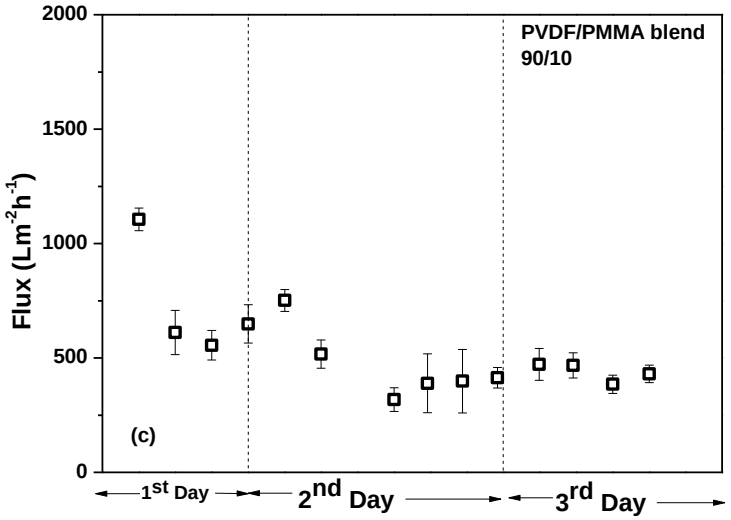

Figure S6: Compaction studies of the (a) 60/40, (b) 70/30 and (c) 90/10 PVDF/PMMA membranes at 30 psi for 3 days.